Luminous Characteristics and ^{89}Y-Static NMR in Red Phosphor, Eu-Doped Y_2O_3

Toshie Harazono,* Etsuzo Yokota, Hiroshi Uchida, and Tokuko Watanabe†

Research Center, Mitsubishi Chemical Co., Ltd., 1000, Kamoshida, Aoba-ku, Yokohama 227

†Tokyo University of Fisheries, 4-5-7, Kounan, Minato-ku, Tokyo 108

(Received September 3, 1997)

Luminous properties of a red phosphor, Eu–Y_2O_3 (Eu-doped Y_2O_3) have been studied by ^{89}Y (nuclear spin 1/2)-static NMR. Pure Y_2O_3 showed an anisotropic pattern with the peak centered at 299 ppm assigned to the Y atom in the site, where none of the 12 nearest neighbouring Y atoms are substituted by an Eu atom. The signal became broader with increasing doped Eu content. Additionally, a shoulder peak assigned to the Y atom in the site where one of the 12 nearest neighbouring Y atoms was replaced by one Eu atom appeared around 100—110 ppm in the samples with more than 1 mol/% Eu content.

The spin–spin relaxation of the centered signal was mainly dominated by the dipole–dipole interaction mechanism between the ^{89}Y nucleus and the paramagnetic electrons of Eu^{3+} with $4f^6$ electron configuration which substituted at the second nearest and further neighbouring Y. In conclusion, the line-broadening of ^{89}Y signal at constant Eu content was correlated with the Eu distribution on the basis of the facts that the phosphor sample with higher brightness showed broader linewidth and the intensity of the ESR signal corresponding to the lattice defects has no relation to the brightness.

Red phosphor, Eu–Y_2O_3 (Eu-doped Y_2O_3), has been used in a projection tube or a lamp having red, blue, and green colors. It is strongly desired that the phosphor is prepared in much smaller particles and has higher brightness because a television tends to be larger. In the phosphors hitherto used, the power of the incident beam of the cathode ray must be increased in order to keep the high brightness with the high resolution on the screen. However, the power of the incident beam is limited because it results in a lowering of the emission efficiency of the phosphor. Therefore, we hope to prepare the phosphor which can realize the high brightness and the high resolution without further increase of incident beam power. In order to develop the phosphor with such characteristics, the crystal field and/or the structure of the emission center must be elucidated. Thus far, component analysis or X-ray analysis has not succeeded in obtaining the data closely related to the characteristics of emission.

Although the limited studies[1—9] of solid state NMR of ^{89}Y (nuclear spin = 1/2 and natural abundance 100%) have been done because of its low resonance frequency, 14.706 MHz at 7.05 T, low sensitivity (1.18×10^{-4} times to ^{1}H), and long spin-lattice relaxation times (several hours), we carried out an investigation by using solid state NMR of Y nuclei to elucidate the distribution of Eu and fine structures of phosphor crystals for the first time.

In this paper, we describe details concerning the dependence of the characteristics of emission efficiency on the Eu distribution and the defects in Y_2O_3. For this purpose, ^{89}Y-static NMR and ESR were employed for the Eu distribution and the defects in Eu–Y_2O_3, respectively.

Experimental

Materials: All the samples used in this study are listed in Table 1. The raw material, Y_2O_3 and Eu_2O_3, were prepared by Mitsubishi Chemical Co., Ltd., and the other materials used as the flux were purchased from Wako Co., Ltd., Junsei Co., Ltd., and Kanto Chemical Co., Ltd. The raw materials, Y_2O_3 and Eu_2O_3, were luminescence grade and all materials purchased were reagent grade.

The samples in this experiment were prepared by the method described in the handbook of phosphors[10] and a patent.[11] The prepa-

Table 1. Sample List of Eu–Y_2O_3

Sample	$(Y_{1-c}Eu_c)_2O_3$		Chroma	Particle size	λ_{max}	Brightness
	$1-c$	c[a)]	x/y[17)]	$d_{50}/\mu m$	nm	%
MR1	1.00	0.00	0.295/0.149	—	380.5	1
MR2	0.99	0.01	0.604/0.361	6.08	611.0	83
MR3	0.97	0.03	0.635/0.354	5.52	611.0	91
MR4	0.95	0.05	0.647/0.349	5.82	611.0	84
MR5	0.93	0.07	0.652/0.345	7.19	611.0	75
MR6	0.90	0.10	0.655/0.343	5.95	611.0	56
MR7	0.70	0.30	0.649/0.342	—	611.0	4
MR8	0.965	0.035	0.640/0.351	3.54	611.0	88
MR9	0.965	0.035	0.642/0.351	5.56	611.0	79
MR10	0.965	0.035	0.640/0.352	3.48	611.0	57
MR11	0.965	0.035	0.638/0.353	4.23	611.0	78
MR12	0.965	0.035	0.641/0.351	4.80	611.0	62
MR13	0.965	0.035	0.637/0.353	3.31	611.0	71

a) Activator content.

ration procedures are as follows. MR1—MR7(Eu-doped Y_2O_3): $BaCl{\cdot}2H_2O$, H_3BO_3, and LiCl were added to Y_2O_3 and Eu_2O_3 as the flux in an alumina crucible and the mixture was heated to 1450 °C and held for several hours to produce Eu-doped Y_2O_3 (Eu–Y_2O_3). MR8: Y_2O_3 and Eu_2O_3 were dissolved in 6 M HCl (1 M = 1 mol dm^{-3}) and 10% oxalic acid solution was added to the solution. By heating up the mixture in an alumina crucible to 1000 °C, the oxalates, $Y_2(C_2O_4)_3$, and $Eu_2(C_2O_4)_3$, were obtained and the following firing at 1450 °C for several hours will produce a co-precipitation Eu–Y_2O_3. MR9—MR13: $BaCl_2{\cdot}2H_2O$, H_3BO_3, and LiCl were added as the flux to the oxalates $Y_2(C_2O_4)_3$ and $Eu_2(C_2O_4)_3$. The mixture was heated to 1450 °C and held for several hours to produce the other co-precipitation Eu–Y_2O_3. All the obtained Eu–Y_2O_3 were washed with pure water several times and dried.

Apparatus and Measurements: Each molar ratio, Eu/Y, and the amounts of impurity were determined by Seiko SPS-1200A ICP and Rigaku 3370 fluorescence X-ray spectrometers. The amounts of impurities of all samples were less than 1 ppm. The activator content was consistent with the analytical concentration of Eu within the experimental error. The crystal structure of Eu–Y_2O_3 was identified in power by an X-ray diffractometer with monochromated Cu K_α (Philips PW1700 diffractometer). The emission spectra and the intensities of brightness were measured with a TOPCON ABT-32 electron-ray emission spectrometer. The particle size was measured with a Model PA-2 coalter counter. The measurements of ^{89}Y-static NMR spectra were carried out at 14.706 MHz on a Bruker MSL-300 spectrometer equipped with a static probe (dia. 10 mm) at room temperature. The 90 ° pulse width was 20 μs and the chemical shifts were determined relatively to 1.5 M $Y(NO_3)_3$ aqueous solution as 0 ppm. A single pulse was used for static measurements. ESR spectra were measured by a JEOL JES-FE2XG ESR spectrometer at room temperature.

Results and Discussion

The schematic diagrams of the crystal structure[12] and of Y–O–Y bonds for Y_2O_3 are shown in Figs. 1-a and 1-b, respectively. In a unit cell (Fig. 1-a), 24Y atoms (24d site, C_2 symmetry),[3] 8Y atoms (8b site, S_6 symmetry),[3] and 48O atoms exist. The X-ray powder diffraction patterns of Eu–Y_2O_3 were almost same as that of the pure Y_2O_3 up to 10 mol% content of Eu. Each Y atom binds 12Y atoms through O atom, as shown in Fig. 1-b. The Y site substituted by the Eu atom is denoted as Y^0; then Y^1, Y^2, ··· are used for the nearest neighboring Y, the second nearest neighboring Y, ··· to the Eu atom. Therefore, the schematic bond is represented as Y^0 (Eu)–O–Y^1–O–Y^2–···. The emission spectrum of Eu–Y_2O_3 showed a sharp strong peak at 611 nm.[10] The pattern of the spectrum was almost the same for Eu–Y_2O_3 with 1 to 10 mol% content of Eu.

ESR Signal: Figure 2 shows the ESR spectrum of MR1 at room temperature. In the spectrum, a sharp peak assigned to F^+ center such that an electron was trapped in an oxygen defect (+2 valent) appeared at $g = 2.004$.[13] Besides the F^+ center peak, several weak signals appeared in the wide magnetic field (ca. 0.23 T). These peaks have not hitherto been assigned. For a series of Eu–Y_2O_3 (MR1 to MR7), the signal intensity of the F^+ center decreased with increase of Eu content, as shown in Fig. 3. In the samples with the same

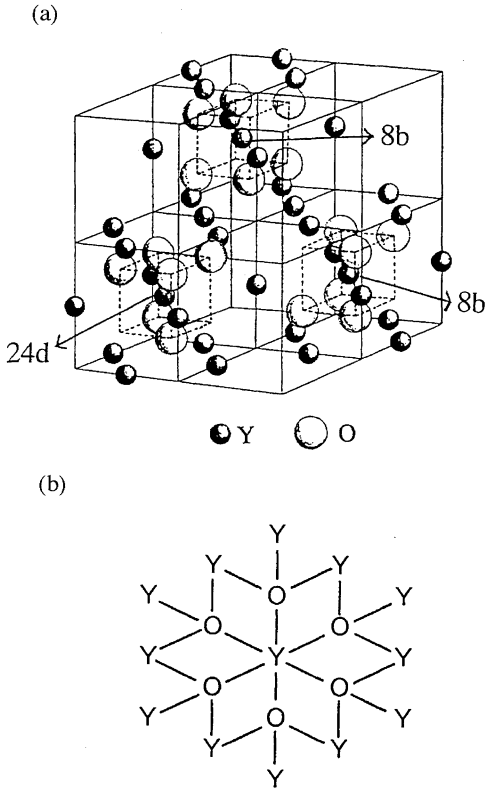

Fig. 1. (a) Schematic crystal structure of Y_2O_3. This diagram shows a unit cell composed of 8 small cubic unit cells (8 octants). 2 of 8 octants take 8b site and 6 of 8 octants take 24d site in accordance with statistical probability. (b) Schematic structure of Y–O–Y bonds for Y_2O_3.

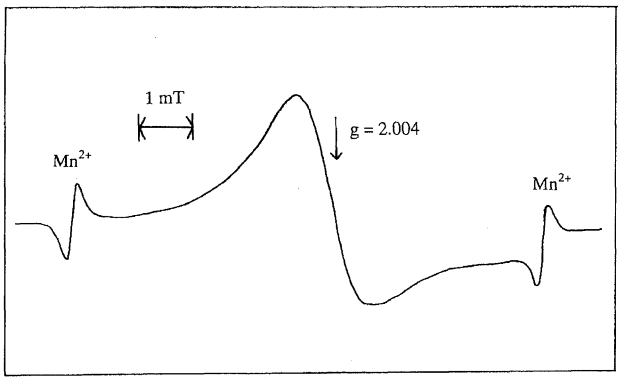

Fig. 2. ESR spectrum of MR1 at room temperature.

Eu content (MR8 to MR13), the signal intensity of the F^+ center became stronger as the particle size decreases.

^{89}Y-Static NMR Spectra: Figure 4-a shows the ^{89}Y-static NMR spectra of Eu–Y_2O_3 with 0 to 10 mol% Eu content (MR1 to MR6). The signal of the sample with 30 mol% Eu content (MR7) was not observed because of the line-broadening. The ^{89}Y-static NMR spectrum of MR1 consists of the superposed peak of ^{89}Y at 24d site ($\sigma_{11} = 399$ ppm, $\sigma_{22} = 299$ ppm, $\sigma_{33} = 282$ ppm) and 8b site ($\sigma_{\parallel} = 352$ ppm, $\sigma_{\perp} = 250$ ppm) and shows the maximum intensity at 299 ppm, corresponding to σ_{22} at 24d site.[1] When Eu atoms were doped in Y_2O_3, the line-broadening of the ^{89}Y signal at

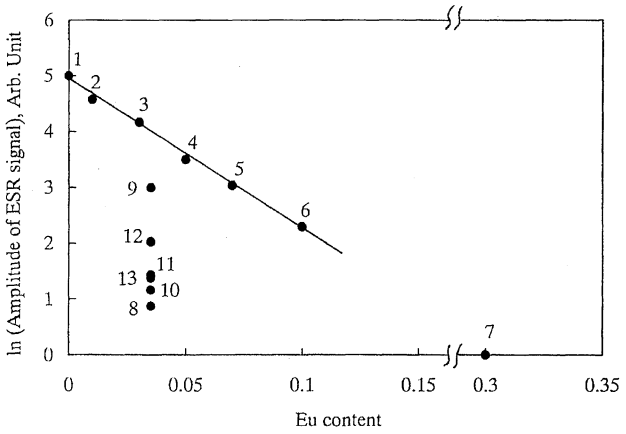

Fig. 3. Plot of ln (I) vs. Eu content. I: amplitude of ESR signal with $g = 2.004$.

299 ppm occurred as observed for MR2 to MR6. As shown in Fig. 1-b, 12(–O–Y) bonds exist around one Y atom. Since the chemical shifts of the main signal in MR2 to MR6 were the same as that in pure Y_2O_3, the signal was assigned to $\underline{Y}(-O-Y, -Y)_6$ where none of the 12 nearest neighboring Y atoms were substituted by Eu atom. The center Y atom in $\underline{Y}(-O-Y, -Y)_6$ is named as Y^A, which exhibits peak A centered at 299 ppm. Eu atoms should be substituted in the second nearest and further neighboring Y to Y^A.

Further, a shoulder peak (B) appeared around 100—110 ppm in MR2 to MR6. Since the shoulder peak became stronger with doping more Eu atoms in Y_2O_3, this peak was attributable to $\underline{Y}(-O-Y, -Y)_5(-O-Y, -Eu)$ where one of the 12 nearest neighboring Y atoms was replaced by one Eu atom. The center Y atom in $\underline{Y}(-O-Y, -Y)_5(-O-Y, -Eu)$ is named as Y^B. The Y^B atom is corresponding to Y^1 with only one nearest neighboring Y site replaced by one Eu atom, abbriviated simply as Y^1(Eu1). The spectra for MR2 to MR6 in Fig. 4-a were deconvoluted to the signal A at 299 ppm and the signal B around 100—110 ppm by employing a gaussian type function, because the line shape of MR2 at 299 ppm was closely approximated by the Gaussian type function. The plots of the difference of the half-width ($\Delta\nu_{1/2}$) of the signals between MR2 to MR6 and MR1, ($\Delta\nu_{1/2}$ (MR2—MR6) – $\Delta\nu_{1/2}$(MR1)), vs. Eu content showed a good correlation, as shown in Fig. 5.

Line-Broadening via Paramagnetic Eu^{3+}: The line-broadening phenomenon of the ^{89}Y signal is expected to be caused by the paramagnetic Eu^{3+} with $4f^6$ electron configuration.[14] If the line-broadening is caused by the dipole–dipole interaction between Y nucleus and the paramagnetic electrons of Eu^{3+}, the next relation is expected.

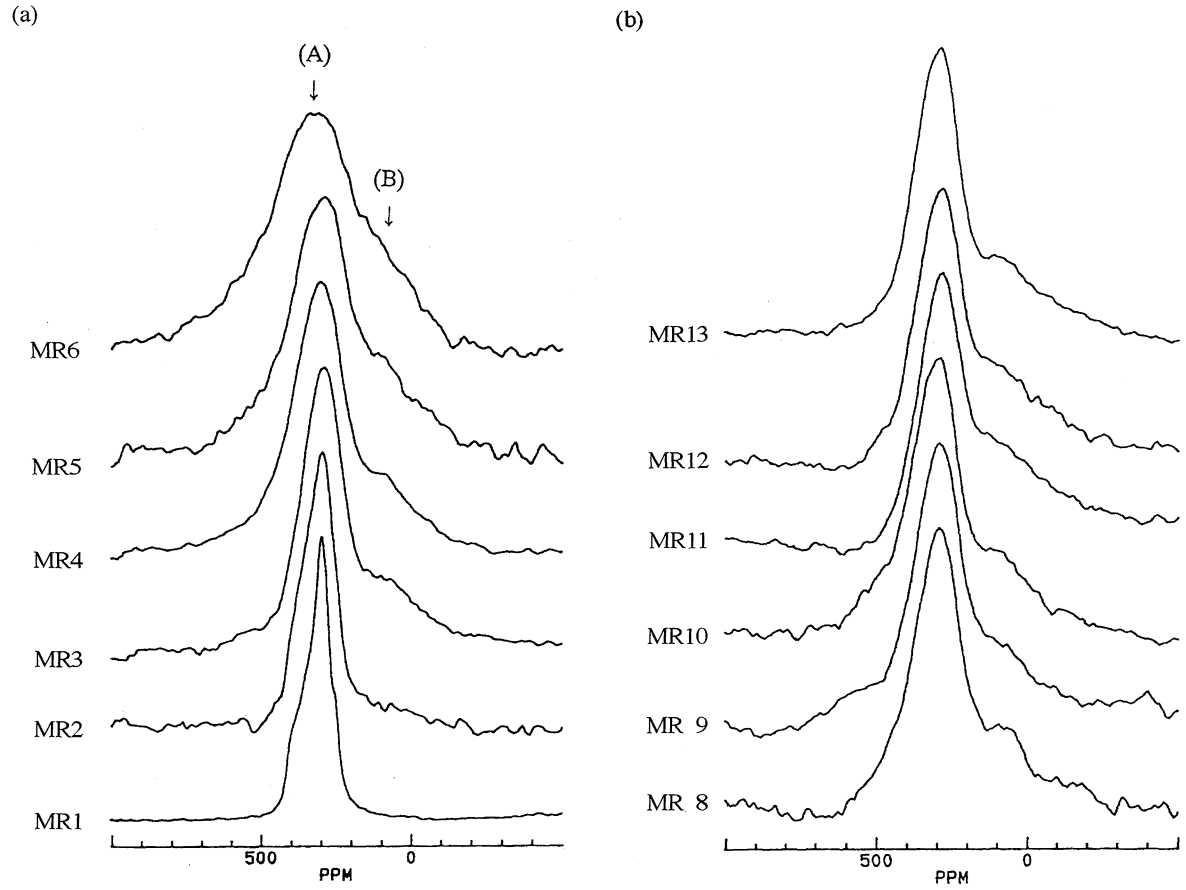

Fig. 4. ^{89}Y-static NMR spectra of MR1 to MR6 (a) and MR8 to MR13 (b). Eu content (mol%): MR1 0%, MR2 1%, MR3 3%, MR4 5%, MR5 7%, MR6 10%, MR8 to MR13 3.5%. Spectral width: 200000 Hz, data point: 4 K, pulse width: 5 μs, aquisition number: 3000—26000, recycle time: 10 s, dead time: 40 μs.

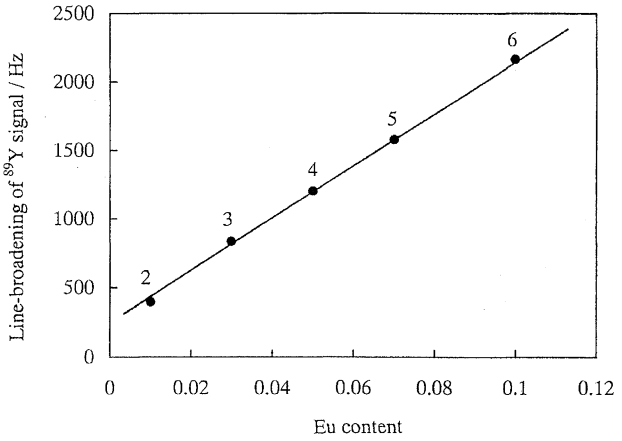

Fig. 5. Line-broadening of the Y^A signal vs. Eu content.

$$\Delta\nu_{1/2} \propto \sum N_j/r_j^3, \quad (1)$$

where r_j is the distance between Y and Eu and N_j is the number of Eu atoms at r_j.

The distances (d) between Y^0 and the nearest neighboring Y^1 in each case are reported as follows:[15] $d(Y^0_{8b}–6Y^1_{24d})$ = 3.516 Å, 3.999 Å, $d(Y^0_{24d}–2Y^1_{8b})$ = 3.516 Å, 4.000 Å, $d(Y^0_{24d}–4Y^1_{24d})$=3.533 Å, 4.014 Å, where the subscript expresses each site, and the coefficient of Y^1 is the number of Y^1 with the same site and distance. The distances between Y^0 and the second nearest neighboring Y^2 scatter in the range of 7 to 8 Å, and the third nearest neighboring Y^3 in the range of 10.5 to 12 Å, depending on the sites. The paramagnetic contribution to Y^A from the Eu atoms substituted at the third nearest neighbor Y^3 and at further Y^3 is thought to be negligible, because the line-broadening is proportional to the inverse of r^3. Therefore, the line-broadening of Y^A is mainly due to the Eu atom substituted at the second nearest neighboring Y^2. Consequently, the number of Eu atoms (effective Eu atoms) which substitute at the second nearest neighboring Y to Y^A in Eq. 1 becomes the main contribution to the linewidth. The line-broadening of signal was proportional to the doped Eu content and became about 5 times, as shown in Fig. 5. This result indicates that the number of Eu atoms substituted at the second nearest neighbouring Y is proportional to that of the doped Eu content for MR2 to MR6 with the same preparation condition.

Relationship between the Line-Broadening of the Y^A Signal and the Brightness: Figure 4-b shows the ^{89}Y-static NMR spectra of MR8 to MR13, which include the same amount of Eu content (3.5 mol%) but were prepared under different preparation conditions such as the firing temperature, firing times, amounts of flux, or total amounts of the raw materials and flux.[11]. The linewidths of the ^{89}Y signals (A) changed depending on the preparation conditions.[11] This phenomenon can be explained by the difference in Eu distribution as described below. One possible image of homogeneous and inhomogeneous distributions of Eu is shown in Figs. 6-a, and -b, respectively. In Fig. 6-b, Y^1(Eu2) indicates the Y^1 with two of the Y^0 sites replaced by Eu atoms, such as $\underline{Y^1}$(–O–Y, –Y)$_4$(–O–Y, –Eu)$_2$, where Y is the nearest

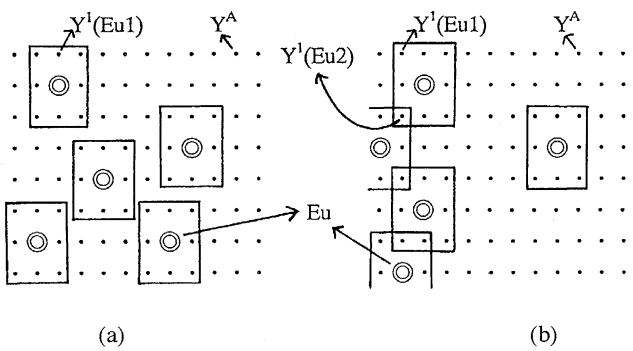

Fig. 6. Models of Eu distributions. (a) homogeneous distribution; (b) inhomogeneous distribution.

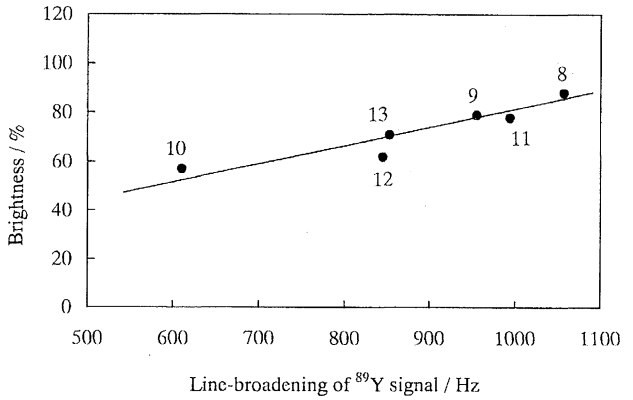

Fig. 7. Plots of the brightness vs. line-broadening of the Y^A signals of MR8 to MR13. Eu content of MR8 and MR13 was kept constant at 3.5 mol%.

neighbouring Y site of Y^1. In other words, Y^1(Eu2) is the Y atom in the site where two of the 12 nearest neighboring Y atoms were replaced by Eu atoms; such a signal cannot be detected because of the line-broadening.[16]

In the homogeneous case (Fig. 6-a), total number of Eu atoms will contribute to the linewidth of Y^A. But in the inhomogeneous case (Fig. 6-b), the number of the second nearest neighboring Y to the doped Eu atom decreases and that of Y^3 and/or further Y^3 increases. Therefore, the apparent content of effective Eu decreases in the inhomogeneous sample. If the total Eu content doped in Y_2O_3 is constant, the number of effective Eu atoms is larger in the homogeneous distribution than in the inhomogeneous distribution. As a result, it is expected that the line-broadening of Y in the homogeneous case becomes larger than that in the inhomogeneous case.

The Eu^{3+} in Y_2O_3 which has $4f^6$ electron configuration emits the red light with λ_{max}= 611 nm as mentioned above. If no path which decreases the brightness is present, the brightness is proportional to the number of Eu atoms. It is generally appreciated that the concentration-quenching effect which decreases the brightness occurs when the Eu–Eu distance becomes shorter.[10] Therefore, it can be suggested that the Eu atoms in the region where Eu atoms are closely distributed do not effectively contribute to the brightness. Therefore, the number of Eu atoms which effectively contributes to the brightness is larger in the homogenous distribution that in the

inhomogeneous distribution, if the total Eu content doped in Y_2O_3 is constant. As a result, Eu–Y_2O_3 with the homogeneous distribution of Eu should exhibit stronger brightness than with the inhomogeneous one at the same Eu content.

Figure 7 demonstrates the relationship between the brightness and the line-broadening of signal A for MR8 to MR13. The brightness became stronger with increasing the line-broadening of the Y^A signal.

Relationship between the Brightness and the Intensity of F^+ Center: The intensities of ESR signals assigned to F^+ center for MR8 to MR13 are shown in Fig. 3. The intensity of F^+ center becomes larger in the order of MR9 > 12 > 11 ≈ 13 > 10 > 8, but the brightness becomes higher in the order of MR8 > 9 ≈ 11 > 13 > 12 > 10. From these results, it is clear that no correlation exists between the intensity of the F^+ center and the brightness.

Conclusions

We investigated the details concerning the relationship between the characteristics of the Eu–Y_2O_3 phosphors, the brightness, and the Eu distribution by using ^{89}Y-static NMR. The relationship between the brightness and the defects was also examined by ESR.

Eu–Y_2O_3 phosphors showed two signals at 299 ppm and at 100—110 ppm. The signal at 299 ppm assigned to $\underline{Y}^A(-O-Y, -Y)_6$, where none of the 12 nearest neighboring Y atoms is substituted by Eu atom, became broader as the doped Eu content increased. The shoulder peak around 100—110 ppm assigned to $\underline{Y}^1(-O-Y, -Y)_5(-O-Y, -Eu)$, where one of 12 nearest neighboring Y atoms was replaced by one Eu atom, appeared in the sample with above 1 mol/% Eu content. The line-broadening of the signal at 299 ppm occurs via the paramagnetic Eu^{3+} with $4f^6$ electron configuration which substituted for the second nearest neighboring and further Y.

From the results that there is a good correlation between line-broadening and brightness and the line-broadening changes depending on the sample preparing conditions, it was proved that the line-broadening of ^{89}Y signal was affected by the Eu distribution, i.e., the linewidth is much broader in the homogeneous distribution than in the inhomogeneous distribution at the same Eu content. Since there was no correlation between the intensity of F^+ center and the brightness, it is concluded that the intensity of brightness would be mainly dominated by the Eu distribution rather than by the amounts of lattice defects.

For obtaining the red phosphor with higher brightness, the sample with highly homogeneous distribution of Eu^{3+} ion should be prepared. This is verified by measurements of linewidth of ^{89}Y-static NMR.

We wish to thank Miss C. Miura (Mitsubishi Chemical Co., Ltd.) for the preparation of compounds investigated.

References

1) T. Harazono and T. Watanabe, *Bull. Chem. Soc. Jpn.*, **70**, 2383 (1997).
2) A. R. Thompson and E. Oldfield, *J. Chem. Soc., Chem. Commun.*, **1987**, 27.
3) P. D. Battle, B. Montez, and E. Oldfield, *J. Chem. Soc., Chem. Commun.*, **1988**, 584.
4) R. Dupree and M. E. Smith, *Chem. Phys. Lett.*, **148**, 41 (1988).
5) A. A. Shemyakov and M. M. Savosta, *Fiz. Tverd. Tela (Leningrad)*, **35**, 236 (1993).
6) G. Balakrishnan, L. W. J. Caves, R. Dupree, D. M. Paul, and M. E. Smith, *Physica C*, **161**, 9 (1989).
7) Z. P. Han, R. Dupree, D. M. Paul, A. P. Howes, and L. W. J. Caves, *Physica C*, **181**, 355 (1991).
8) C. P. Grey, M. E. Smith, A. K. Cheethan, C. M. Dobson, and R. Dupree, *J. Am. Chem. Soc.*, **112**, 4670 (1990).
9) K. J. D. MacKenzie and R. H. Meinhold, *J. Mater. Chem.*, **4**, 1595 (1994)
10) "Handbook of Phosphors," ed by Phosphor Research Society, Ohm Co., Ltd., p. 168 (preparation), p. 229 (emission spectrum), p. 78 (concentration quenching), Tokyo (1987).
11) T. Harazono, E. Yokota, H. Uchida, A. Hase, and C. Miura, "Yttrium Oxide Phosphor," Japan Patent 127773-1996, p. 1—6.
12) F. S. Galasso, "International Series of Monographs in Solid State Physic," Pergamon Press Ltd., Vol. 7, "Structure and Properties of Inorganic Solids," p. 102, Oxford (1970).
13) M. Tamatani, T. Tsuda, K. Nomoto, T. Nishimura, and K. Yokota, *J. Lumin.*, **12/13**, 935 (1976).
14) A. Abragam, "Principles of Nuclear Magnetism," Clarendon Press, Oxford (1961), Chap. 9.
15) M. Faucher, *Acta Crystallogr., Sect. B*, **B36**, 3209 (1980).
16) This phenomenon has been confirmed by ^{89}Y-MAS NMR spectra. We are preparing a separate paper.
17) Specification of Colors according to the Commision Internationale de l'Eclairage (CIE) 1931. "JIS Handbook 33, "Colors" Z8701-1982," ed by Japan Society of Standard, p. 117.